Hindawi Publishing Corporation
Mathematical Problems in Engineering
Volume 2014, Article ID 570161, 10 pages
http://dx.doi.org/10.1155/2014/570161

Review Article

Overview of Bearingless Induction Motors

Xiaodong Sun,[1] Long Chen,[1] and Zebin Yang[2]

[1] *Automotive Engineering Research Institute, Jiangsu University, Zhenjiang 212013, China*
[2] *School of Electrical and Information Engineering, Jiangsu University, Zhenjiang 212013, China*

Correspondence should be addressed to Xiaodong Sun; xdsun@ujs.edu.cn

Received 21 September 2013; Accepted 5 February 2014; Published 9 March 2014

Academic Editor: Ivo Doležel

Bearingless induction motors combining functions of both torque generation and noncontact magnetic suspension together have attracted more and more attention in the past decades due to their definite advantages of compactness, simple structure, less maintenance, no wear particles, high rotational speed, and so forth. This paper overviews the key technologies of the bearingless induction motors, with emphasis on motor topologies, mathematical models, and control strategies. Particularly, in the control issues, the vector control, independent control, direct torque control, nonlinear decoupling control, sensorless control, and so forth are investigated. In addition, several possible development trends of the bearingless induction motors are also discussed.

1. Introduction

The idea of bearingless motors can be traced back to 1973 when Hermann proposed probably the first radial active magnetic bearing topology [1], in which two sets of windings are embedded in the stator so as to produce the driving moment and radial strength simultaneously. In 1988, Swiss scholar Bosch first proposed and used the "bearingles *sic* motor" concept [2]. Since then, there is a fast growing interest in bearingless motor, and the concept has been reported in various publications on magnetic levitation. The importance of bearingless motors is related to the integration of the drive control of the electrical motor and the suspension control of its rotor in a compact volume. Generally speaking, the principal characteristic of bearingless motors is the existence of two kinds of stator windings, and one assists in the torque generation and the other one for the rotor suspension. Compared with the well-known magnetic bearing driving topology of the electrical motor and independent magnetic bearings mounted in the same axis, the advantages of the bearingless motor are compactness, a simple structure, and cost reduction.

So far, various types of motors have been put forward as bearingless motors, such as synchronous reluctance [3, 4] and switched reluctance types [5, 6], induction type [7, 8], surface mounted permanent magnet (PM) [9, 10], inset PM [11], interior and buried PM types [12], Lorentz slotless type [13, 14], consequent-pole type [15, 16], and brushless DC type [17, 18]. Among these types of bearingless motors, the bearingless induction motor is being actively researched and developed around the word since it possesses the following advantages.

(1) Its rotor topology is relatively simple and robust.

(2) It provides nearly constant rotational speed.

(3) Its torque ripples and cogging torque are less.

(4) The cost is low for open loop operation.

Being continually fueled by new motor topologies and control strategies, bearingless induction motors are becoming more and more attractive and have been identified to be one of the most promising motors for the special industrial applications.

The purpose of this paper is to give an overview of the bearingless induction motors. Thus, the state-of-the-art technology of bearingless induction motors, including operation principles, motor topologies, mathematical models, control strategies, and latest development trends, will be reviewed and discussed.

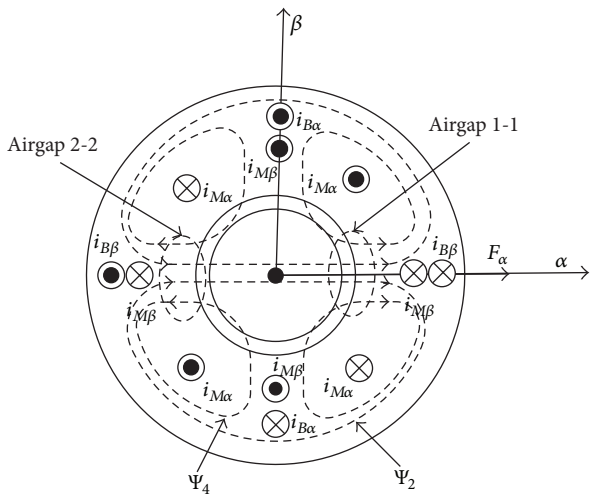

Figure 1: Principle of radial suspension forces generation.

2. Principle of Radial Suspension Force Generation

The basic winding configuration of a bearingless induction motor in the stationary perpendiculars α- and β-axes is shown in Figure 1. Two sets of windings are wound in the same stator slots. One is the 4-pole windings for the production of the torque. The other is the 2-pole windings for the production of the radial suspension force so as to control the rotor radial position in the airgap. These windings are referred as the torque and suspension force windings, respectively.

The main 4-pole flux Ψ_4 is generated by torque winding current $i_{M\alpha}$. Under no-load balanced conditions, if a positive radial suspension force along the α-axis is needed, the suspension force winding current $i_{B\alpha}$ is fed as shown in Figure 1. The flux density in the airgap 1-1 is increased, because both Ψ_2 and Ψ_4 fluxes are in the same direction. On the other hand, the flux density in the airgap 2-2 is decreased because Ψ_2 and Ψ_4 are in the opposite direction. A positive suspension force F_α is produced in the α-axis direction only. The reverse current can produce the opposite radial suspension force. The radial suspension force F_β in the β-axis direction can be produced using electrically perpendicular 2-pole suspension force winding current $i_{B\beta}$ distribution.

3. Motor Topologies

3.1. 2 Degrees of Freedom (DOF) Bearingless Induction Motor. At present, the bearingless induction motor topologies are mainly concentrated in the 2-DOF 3-phase squirrel cage type bearingless induction motors which are usually used as principle prototypes in the laboratory. However, the standard squirrel cage rotor will cause problem when it is used in a bearingless induction motor to produce the radial suspension force. As known, a sudden change in the radial suspension force will lead to a sudden change of the stator flux of the suspension force winding. The rotor flux, however, does not change suddenly, because the voltage is induced into the rotor circuit, which generates the rotor current. Therefore, the interaction of stator and rotor circuits will engender a delay in the flux of the suspension force winding which in turn delays the radial suspension force response.

In order to conquer the problem associated with the conventional squirrel cage rotor, Chiba and Fukao [19] proposed a novel bearingless induction motor with an optimal designed rotor circuits. The proposed bearingless induction motor with 4-pole torque and 2-pole suspension force windings has a 4-pole pole-specific rotor short circuit. Four rotor bars are connected by four end-ring segments (rather than complete rings) so that a 4-pole circuit is constructed. If a 4-pole rotating magnetic field of the torque winding is applied, the circulating current is generated in the short circuits. However, there is no current when a 2-pole rotating magnetic field of the suspension winding is applied because the EMFs induced into the circuits sum to zero. Therefore, there is no mutual inductance between the rotor and suspension force windings, and the radial suspension force is also not influenced by the induced rotor current.

In the 2-DOF bearingless induction motors, the motors with two sets of windings, one for generating torque and another for producing the radial suspension forces, are primarily researched. Besides, Ribeiro et al. [20] proposed another structure of the bearingless induction motor, in which the 3-phase windings of a 4-pole off-shelf induction motor are splitting into two sets of 3-phase windings and its midpoint is grounded. The corresponding configuration of the split-phase bearingless induction motor drive system is shown in Figure 2, in which there are six windings, namely, windings a, b, and c and windings $-a$, $-b$, and $-c$. The radial suspension force can be generated by using a phase current deviation parcel Δi in a group of two windings in the same direction. For instance, if a positive radial suspension force along the y-axis is needed, the windings a and $-a$ are fed as presented in Figure 2. In this condition, the motor phase currents for the rotor levitation scheme can be expressed as $i_a + \Delta i$ and $i_a - \Delta i$. The asymmetry caused by the introduction of Δi produces a resultant force in the y-axis. In comparison to the traditional bearingless induction motor with the structure of double windings, the split-phase bearingless induction motor with the single set of winding has the advantages of simple structure, low power loss, low cost, and so forth. However, it requires a nonstandard control strategy to accomplish a suitable motor operation.

As it is well known, the multiphase motor, with phases number not less than 5, has the multiple orthogonal d-q planes. One d-q plane can be utilized for the torque control, and the other d-q planes can be used in a different manner. Based on this theory, Huang et al. [21] introduced the multiphase motor technology into the single winding bearingless induction motor and proposed a 5-phase bearingless induction motor with multiphase windings, which can generate two needed rotating magnetic fields by feeding two groups of currents to the single set of multiphase windings by using a multiphase converter. The 5-phase windings have the same structure, and each of them is 72° displaced in angular space around the motor stator. In the proposed bearingless induction motor, one d-q plane is used for the motor drive

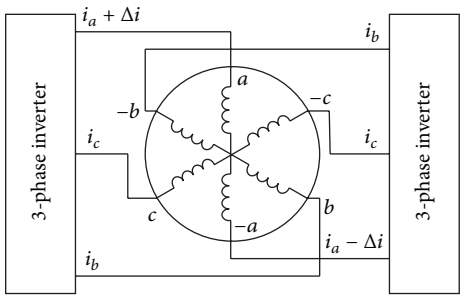

Figure 2: Configuration of the split-phase bearingless induction motor drive system [20].

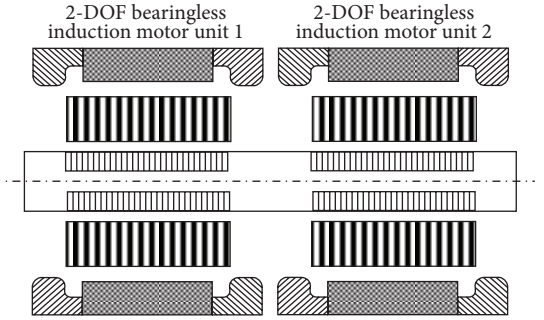

Figure 3: Structure diagram of 4-DOF bearingless induction motor.

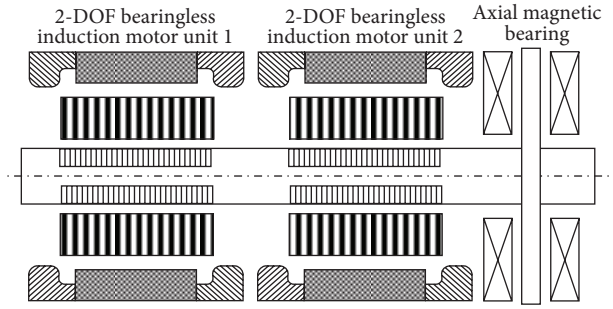

Figure 4: Structure diagram of 5-DOF bearingless induction motor (one structure) [23].

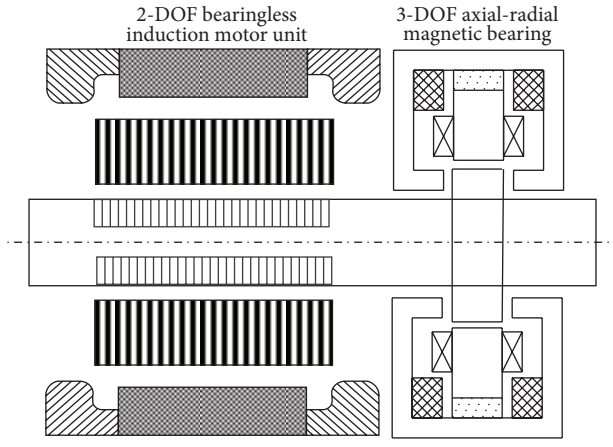

Figure 5: Structure diagram of the 5-DOF bearingless induction motor (another structure) [24].

control, and the other d-q plane is utilized for the rotor levitation control. The proposed motor not only has the advantages of a simpler structure and low power switch loss of bearingless motors with a single set of windings, but also possesses advantages of high power ratings with lower voltage limited devices of the multiphase motors. In addition, the proposed motor also has the redundant features, and it is most viable for fault-tolerant operation.

3.2. 4-DOF Bearingless Induction Motor. As stated earlier, the 2-DOF bearingless induction motors are primarily used in the laboratory as the principle prototypes. It is worth to mention that evaluating the performance of the rotor levitation as well as electric motor characteristics is necessary for them to apply in the practical application. In [22], Chiba et al. proposed a 4-DOF bearingless induction motor, and its structure diagram is shown in Figure 3. The 4-DOF bearingless induction motor consists of two tandem 2-DOF bearingless induction motor units. The units 1 and 2 regulate the radial shaft positions of the left and right shaft ends, respectively. In each unit, two sets of 3-phase windings are arranged in the stator core. One is for motor torque control, and the other is for radial suspension force control. And the rotating magnetic field can guarantee the horizontal shaft position stable passively. In the experimental platform, a rotor resistance identification method was introduced and corresponding controller strategy was designed. Finally, the experimental studies were carried out, and the results confirmed that the proposed control strategy for rotor resistance identification is effective in compensating the adverse effects of temperature increase for the stable operation of the 4-DOF bearingless induction motors.

3.3. 5-DOF Bearingless Induction Motor. In Figure 3, the 4-DOF bearingless induction motor is split into two 2-DOF bearingless induction motors, which together provide the total torque and 2-DOF radial suspension of the rotor in the left and right shaft ends, respectively. In case of big axial suspension forces or strict requirements to axial positioning, an axial magnetic bearing needs to be added. In [23], Santisteban et al. proposed a 5-DOF bearingless induction motor consisting of two 2-DOF bearingless induction motor units and an axial magnetic bearing unit as shown in Figure 4. Besides some advantages, for example, low friction and low maintenance, the 5-DOF bearingless induction motor has many disadvantages, such as complex mechanical structure, increased shaft length, limited critical rotor speed, reduced shaft resonance frequencies, need for special iron laminations, and dc choppers, which increase system complexity and cost. In addition, synchronization control between the two 2-DOF bearingless induction motors is indispensable, which results in the complicated decoupling control system.

In view of the insufficient of the 5-DOF bearingless induction motor proposed in [23], an innovative 5-DOF bearingless induction motor, consisting of a 2-DOF bearingless induction motor and a 3-DOF axial-radial magnetic bearing, is proposed in [24], as shown in Figure 5. Since the 3-DOF combined axial-radial magnetic bearing with permanent

magnet bias excitation possesses the ability of integrating the axial and radial suspension forces generation into one unit, the axial length of the rotor is reduced, and the axial utilization rate is increased, which further promote the critical speed and power density the of the 5-DOF bearingless induction motor.

4. Mathematical Model

The mathematical models, including electromagnetic torque and radial suspension force equations, are the theoretical foundation of the bearingless induction motor. Obtaining the accurate mathematical expressions of the electromagnetism torque and the radial suspension force is critical to realize the stable suspension operation of the bearingless induction motor.

4.1. Radial Suspension Force Model. Basically, the method of calculating the radial suspension force can be classified as two kinds of methods virtual displacement method [4, 8, 22, 26] and Maxwell tensor method [27–29].

4.1.1. Virtual Displacement Method. The inductance matrix [**L**] of two sets of the windings of the bearingless induction motor can be derived according to the equivalent magnetic circuit principle, which are given by

$$[\mathbf{L}] = \begin{bmatrix} L_M & 0 & -Mx & My \\ 0 & L_M & My & Mx \\ -Mx & My & L_B & 0 \\ My & Mx & 0 & L_B \end{bmatrix}, \tag{1}$$

where L_M and L_B are self-inductances of torque and suspension force windings, respectively, M is the mutual inductance coefficient of torque and suspension force windings, and x and y are the rotor radial displacement in the x- and y-directions, respectively. Subscripts M and B correspond to torque winding and suspension force winding, respectively (the same hereafter). And the current matrix [**i**] of the torque and suspension force windings can be written as

$$[\mathbf{i}] = \begin{bmatrix} i_{Md} & i_{Mq} & i_{Bd} & i_{Bq} \end{bmatrix}^T, \tag{2}$$

where i_{Md} and i_{Mq} are current components of torque windings in d-q coordinate, respectively, and i_{Bd} and i_{Bq} are current components of suspension force windings in d-q coordinate, respectively. And then, the expression of the electromagnetic energy is gotten according to the energy conversion relationship, which is written as

$$W_m = \frac{1}{2}[\mathbf{i}]^T [\mathbf{L}] [\mathbf{i}]. \tag{3}$$

Finally, the model of the radial suspension force can be obtained by the virtual displacement method, which is expressed as

$$\begin{bmatrix} F_x \\ F_y \end{bmatrix} = \begin{bmatrix} \dfrac{\partial \mathbf{W}_m}{\partial x} \\ \dfrac{\partial \mathbf{W}_m}{\partial y} \end{bmatrix} = M \begin{bmatrix} -i_{Md} & i_{Mq} \\ i_{Mq} & i_{Md} \end{bmatrix} \begin{bmatrix} i_{Bd} \\ i_{Bq} \end{bmatrix}. \tag{4}$$

4.1.2. Maxwell Tensor Method. The airgap magnetic flux density of the bearingless induction motor is collectively produced by the torque and suspension force windings, and it can be written as

$$B(\varphi) = B_M \cos(p_M \varphi - \omega_M t + \mu) + B_B \cos(p_B \varphi - \omega_B t + \lambda), \tag{5}$$

where φ is the space position angle, μ and λ are initial phase angles of torque and suspension windings, respectively, and B_M and B_B are the amplitude of the airgap magnetic flux density of torque and suspension windings, respectively. For the airgap flux density B, the Maxwell force element which acts on a surface element dA of the rotor can be expressed as

$$dF = \frac{B^2}{2\mu_0} dA, \tag{6}$$

where μ_0 is the vacuum magnetic permeability and dA is the infinitesimal surface element of the rotor.

By integrating (6), when $p_B = p_M + 1$, the Maxwell forces in the x- and y-directions can be given as

$$\begin{aligned} F_x &= F_M \cos(\lambda - \mu) \\ F_y &= F_M \sin(\lambda - \mu), \end{aligned} \tag{7}$$

where p_M and p_B are the pole-pair numbers of torque and suspension force winding, respectively, F_x and F_y are the Maxwell forces in x- and y-direction, respectively, $F_M = lr\pi B_M B_B / 2\mu_0$ is the amplitude of Maxwell force, l is the active core length, and r is the rotor outer radius.

The airgap flux linkage of torque and suspension force windings can be expressed as

$$\begin{aligned} \Psi_M &= \frac{2lrB_M N_M}{p_M}, \\ \Psi_B &= \frac{2lrB_B N_M}{p_B} \approx L_{mB} i_B, \end{aligned} \tag{8}$$

where L_{mB} is the mutual inductance of the suspension force windings and N_M and N_B are number of turns of the torque and suspension force windings, respectively.

Based on the vector multiplication operation, (7) can be expressed in the d-q rotating coordinate as

$$\begin{aligned} F_x &= k_M \left(i_{Bd} \Psi_{Md} + i_{Bq} \Psi_{Mq} \right), \\ F_y &= k_M \left(i_{Bq} \Psi_{Md} - i_{Bd} \Psi_{Mq} \right), \end{aligned} \tag{9}$$

where $F_M = \pi p_M p_B L_{mB} / 2lr\mu_0 N_M N_B$, Ψ_{Md}, and Ψ_{Mq} are the airgap flux linkages components of torque windings in d-q coordinates, respectively and Ψ_{Bd} and Ψ_{Bq} are the airgap flux linkages components of suspension force windings in d-q coordinates, respectively.

In the process of practical operation, the eccentricity of the stator and rotor is inescapable, which will lead to complex analysis and computation of the radial suspension force. In order to improve the control precision of the radial suspension force, an accurate radial suspension force expression

considering the rotor positioning eccentricity was established [30], which is suitable for real-time computation in rotor suspension control application. In addition, the computation accuracy of the proposed radial suspension force model was verified by the Finite Element (FE) analysis. And then, a novel radial suspension force feedback control method for the bearingless induction motor was proposed on the basis of the aforementioned radial suspension force model, and corresponding simulation studies were carried out. The research results indicated that the proposed radial suspension force model as well as the corresponding control strategy could improve the radial positioning control accuracy of the rotor markedly and enhance the overall static and dynamic behaviors of stable suspension operation obviously for the bearingless induction motor.

4.2. Electromagnetic Torque Equation. In comparison to the magnetic field produced by torque windings, the magnetic field produced by suspension force windings is so small that it can be ignored. So the airgap flux linkages equation of the torque windings can be expressed as

$$\begin{aligned} \Psi_{Md} &= L_{mM}\left(i_{Md} + i_{Mrd}\right), \\ \Psi_{Mq} &= L_{mM}\left(i_{Mq} + i_{Mrq}\right), \end{aligned} \tag{10}$$

where i_{Mrd} and i_{Mrq} are rotor current components of torque windings in d-q coordinate, respectively. And the electromagnetic torque equation can be written as

$$T_e = p_M\left(i_{Mq}\Psi_{Md} - i_{Md}\Psi_{Mq}\right). \tag{11}$$

5. Control Strategies

5.1. Vector Control. The vector control (VC) strategy includes airgap flux oriented control and rotor flux oriented control, and in this section, the rotor flux oriented control for the bearingless induction motor is presented as an example.

When the rotor flux oriented control method is adopted, the rotor flux vector of torque windings is aligned with d-axis, which means that the rotor flux linkages components of torque windings can be given as $\Psi_{Mdr} = \Psi_{Mr}$ and $\Psi_{Mqr} = 0$. Then the torque winding currents i_{Md} and i_{Mq}, the slip angular speed ω_s, and the electromagnetic torque T_e can be expressed as

$$\begin{aligned} i_{Md} &= \frac{L_{Mr}p_M + 1}{R_{Mr}L_{mM}}\Psi_{Mr}, \\ i_{Mq} &= \frac{T_e L_{Mr}}{p_M L_{mM}\Psi_{Mr}}, \\ \omega_s &= \frac{R_{Mr}L_{mM}}{L_{Mr}\Psi_{Mr}}i_{Mq}, \\ T_e &= p_M\frac{L_{mM}}{L_{Mr}}i_{Mq}\Psi_{Mr}, \end{aligned} \tag{12}$$

where L_{Mr} and R_{Mr} are the rotor inductance and resistance of torque windings, respectively, Ψ_{Mdr} and Ψ_{Mqr} are rotor flux linkages components of torque windings, respectively, and L_{mM} is the mutual inductance of torque windings.

From (9), we can see that the radial suspension forces are related to the airgap flux linkages of the torque windings. Therefore, only after the airgap flux linkages are obtained they can be used to calculate the radial suspension forces. In view of the relationship between airgap flux and rotor flux linkages, the rotor flux linkages and stator currents of torque windings are used to identify the airgap flux linkages, which can be expressed as

$$\begin{aligned} \Psi_{Md} &= \frac{L_{mM}}{L_{Mr}}\left(\Psi_{Mdr} + L_{Mrl}i_{Md}\right), \\ \Psi_{Mq} &= \frac{L_{mM}}{L_{Mr}}L_{Mrl}i_{Mq}, \end{aligned} \tag{13}$$

where L_{Mrl} is the rotor leakage inductance of the torque windings. After the airgap is obtained, the suspension force winding currents can be determined in accordance with (9). By solving (9), we obtain

$$\begin{bmatrix} i_{Bd} \\ i_{Bq} \end{bmatrix} = \frac{1}{k}\begin{bmatrix} \cos\rho & -\sin\rho \\ \sin\rho & \cos\rho \end{bmatrix}\begin{bmatrix} F_x \\ F_y \end{bmatrix}, \tag{14}$$

where $k = K_M\sqrt{\Psi_{Md}^2 + \Psi_{Mq}^2}$ and $\rho = \arctan(\Psi_{Mq}/\Psi_{Md})$. The control block diagram of the rotor flux oriented control is shown in Figure 6.

5.2. Independent Control. Radial suspension force and torque are the control objectives that determine the machine performance of levitation and rotation in a bearingless induction motor. However, from (9), it can be seen that the information in regards to the airgap flux linkages of the torque windings is crucial for the radial suspension force control. As for the VC, there is the time delay of the information transmission between torque control and radial suspension force control systems, which leads to the restriction between the control schemes of torque and suspension force windings and further affects the whole control performance of bearingless induction motor drives. To effectively avoid the disadvantage, the independent control (IC) strategy for the bearingless induction motor was proposed [25] and the corresponding control block diagram is shown in Figure 7. The airgap flux linkage of the torque windings can be identified by using the conventional voltage-current model, which can realize the torque and radial suspension force separately controlled by different variables, and hence simplifying the control algorithm of the torque winding.

5.3. Direct Torque Control. Direct torque control (DTC) is a powerful and attractive control strategy with a simple structure, fast behavior, and tolerance to the variation of motor parameters, which offers direct and effective control of stator flux and torque by optimally selecting the inverter switch states in each sampling period. The DTC method provides a systematic solution for improving the operating characteristics of the motor as well as the voltage source inverter. In order to overcome the limitations such as complexity, unsteady

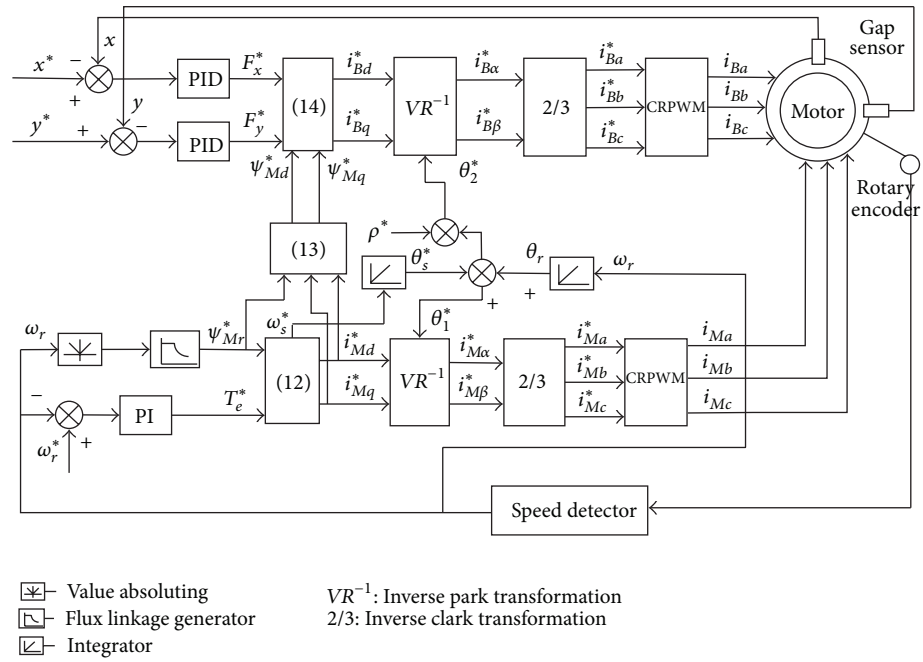

Figure 6: Control block diagram of the rotor flux oriented control.

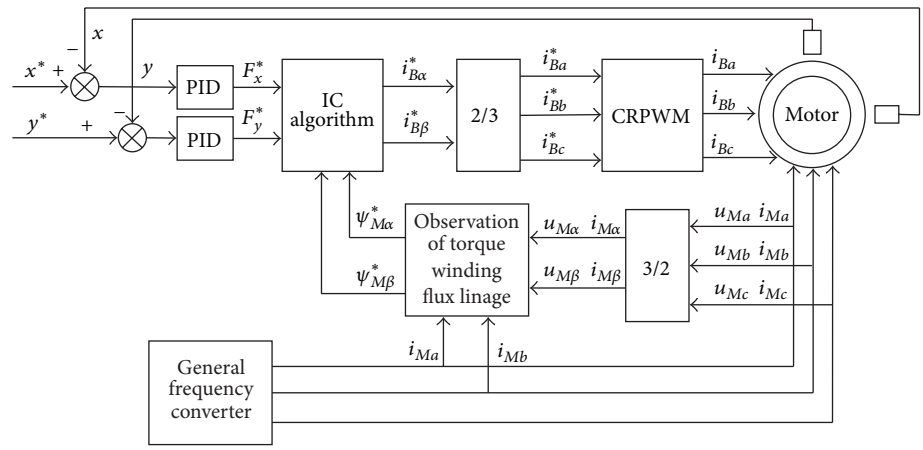

Figure 7: Control block diagram of the IC [25].

torque, and nonlinearity in the VC algorithm, Wang et al. proposed a space vector pulse width modulation (SVPWM-) based DTC method for the bearingless induction motor drives [31]. The small signal model of Maxwell force was adopted to analyze the influence of the current ripple of torque windings on radial suspension force. The outputs of the torque PI and flux PI modulators, namely, flux phase angle and amplitude increments, provided proper voltage vectors via the inverter in such a way that these two variables were forced to be predefined trajectories. In addition, a regulator for phase angle increment was also adopted to solve the disturbance problems in torque and flux loops. The experimental results have validated that the proposed algorithm has a better performance in reducing disturbances of current and torque, and hence improving the suspension performance of the bearingless induction motor.

5.4. Nonlinear Decoupling Control. The bearingless induction motor is a multivariable, nonlinear, and strong coupled system, which makes the control of the whole system more complex. To realize the bearingless induction motor suspension operation steadily and reliably, it is necessary to achieve the nonlinear decoupling control (NDC) between torque and radial suspension forces independently. As for the decoupling control of the bearingless induction motor, the traditional approach is the VC method. Its control performance is acceptable when the rotor always suspends at the center of the airgap. Moreover, the VC method is essentially a steady-state decoupling control, which can only achieve the decoupling control between radial suspension forces and electromagnetic torque but cannot realize the dynamic decoupling control of them. Therefore, the dynamic response performance is not satisfactory.

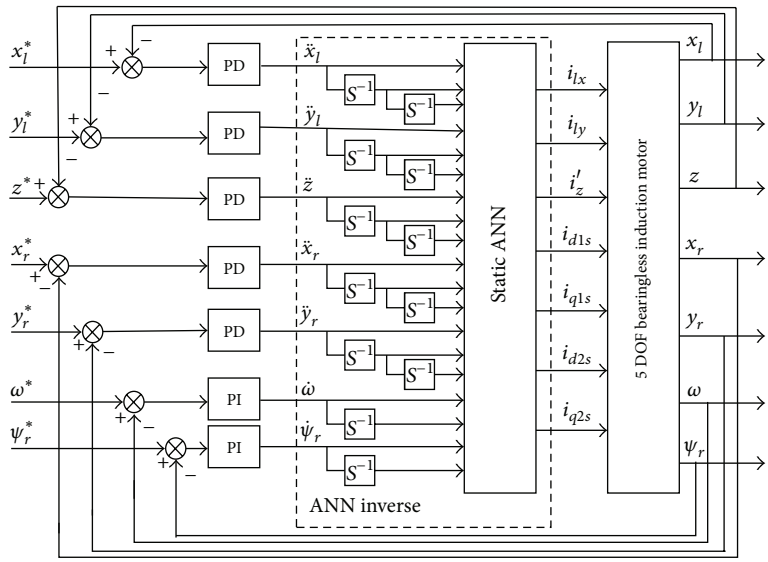

Figure 8: Control block diagram of the ANNI method [24].

In [32], the inverse system method is proposed by Zhu et al. for the nonlinear decoupling control of the bearingless induction motor. By applying the inverse method, the bearingless induction motor system is decoupled into two 2-order linear displacement subsystems, a 1-order linear speed subsystem, and a 1-order linear magnetic linkage subsystem. Based on this, the linear control techniques were applied to design the close-loop regulators of these pseudo-linear systems. However, the decoupling and the linearization of multivariate nonlinear system with the inverse system method demand a precise mathematical model of the controlled object. Since there are some uncertain nonlinear factors in the practical operation, such as load disturbance, rotor eccentricity, and rotor parameter variation, a high-precision, fast-response control is not easy to be achieved by the inverse system approach.

As it is well-known, the static artificial neural network (ANN), such as radial basis function network and multilayer neural network, has the ability to learn and self-adapt, approximate any arbitrary nonlinear mapping, and have the effective control to complex and uncertain system. Taking the advantage of approximating ability of the static ANN, a kind of continuous dynamic ANN structure was formed in [24] by introducing integrators to a static ANN, and then the ANN inverse (ANNI) method was proposed for the nonlinear decoupling control of the 5-DOF bearingless induction motors. The static ANN is adopted to approach the inversion of the bearingless induction motor, and the integrators are used to characterize its dynamic characteristics. The corresponding control diagram of the ANNI method is shown in Figure 8.

5.5. Sensorless Control. Similar to the conventional induction motors, the rotor position information, which is traditionally measured by a physical sensor, is mandatory for the proper operation of the bearingless induction motor. In addition, the mechanical displacement sensors are also indispensable for the stable suspension operation. In order to avoid some difficulties resulting from the traditional sensor control method and effectively reduce the cost and short a shaft length, the sensorless control (SC) of bearingless induction motor was implemented [33]. The proposed SC method is based on the detection of currents induced by mutual inductances, which vary as a function of the rotor radial displacements. By superimposing a high-frequency carrier voltage on the torque windings, the induced carrier-frequency current component is obvious from the suspension force winding current. Moreover, a simple current estimator is designed to eliminate the carrier-frequency component originated from the transient voltage of the suspension force windings.

5.6. Comparison of Control Strategies. The main advantages, major disadvantages, and typical techniques of the aforementioned control strategies are compared, and the corresponding conclusions are summed up as shown in Table 1. As for the NDC, the ANNI control is used for exemplification as an example.

6. Development Trends

In this section, several emerging development trends of the bearingless induction motor are identified and discussed.

6.1. Prototype Structure. Generally, to make the bearingless induction motor drives satisfy the requirements of engineering application, it is necessary to achieve the suspension control of the radial 4-DOF and axial single-DOF control of the rotor. The aforementioned two kinds of the 5-DOF bearingless induction motors must be configured with magnetic bearings, which increases the axial length of the rotor and the reactive power losses of the system and restricts the enhancement of the critical speed and the system efficiency. Therefore, an intensive study on designing novel 5-DOF bearingless induction motor prototype structure with a

Table 1: Comparison of control strategies.

	Advantages	Disadvantages	Techniques
VC	Realizing easily; no special requirements for hardware and software	Causing coupling between two sets of the windings	Generating the current control signals using the feedback and coordinate transformation
IC	Achieving IC of radial suspension force, and hence improving the flexibility of torque control scheme	Requiring additional magnetic flux observer	Obtaining the torque winding flux linage dependently
DTC	Fast torque response; less parameter dependence; no need for current control	Causing errors due to variation of stator resistance and drift in flux linkage estimation	Generating the voltage vectors using independent torque and flux computations
NDC	Flexible control algorithms; adapting nonlinear theories and parameter variations	Requiring sophisticated hardware and intensive computation or experiential knowledge	Taking advantage of neural network or other nonlinear theory
SC	Removing the mechanical sensors, and hence reducing the system cost and size; readily merging into other controls	Requiring sophisticated hardware and intensive computation	Estimating the position and displacement based on the motor mutual inductance

simple motor topology, low power losses, and high efficiency is of great practical significance.

6.2. Advanced Control. As for the control strategies of the suspension force windings, the most common method is the radial displacement negative feedback modulation-based control strategy, which requires the complicated force/current transformation and coordinate transformations. As a result, the algorithm is more complex, which seriously influence the dynamic response and anti-interference ability of the bearingless induction motors. Therefore, it is necessary to develop the new control strategy for the suspension control of the rotor. Among these control algorithms, the direct radial suspension force control, which can be inspired by the DTC method, will be the next research hot spot of the radial suspension force control for the bearingless induction motors.

6.3. Sensor Integration and Sensorless Technologies. Current, speed, displacement, and temperature sensors, which are the very important part of the drive system for bearingless induction motors, play an important role for the table suspension operation of the whole system. However, these sensors are also the potential fault hidden troubles, since after long-time use they cause problems and then lead to the misoperation and malfunction of the whole control system. In this case, the sensorless technologies may be the preferred solution. Although some sensorless technologies have been proposed separately for the position or displacement detection by international and domestic academics and experts, the position and displacement sensorless operation of bearingless induction motor was still investigated separately, which cannot realize the integrated self-sensing of the rotor position and displacement. Therefore, to do some research to implement the integrated sensorless suspension operation, the function integration of the prototype and sensors has important practical significance and theoretical value.

6.4. Reliability Technology. Reliability is one of the most critical requirements in some special applications, such as turbomolecular pumps, canned pumps, and centrifugal machines, where a continuous operation must be ensured. Under the premise of satisfying each performance index of the bearingless induction motors, the study on developing the redundant or conservative design techniques and the fault-tolerant control strategies, so as to reduce or avoid the unnecessary losses caused by the failures, has very important practical meaning and is also an important issue for the researchers in this field.

7. Conclusion

In this paper, the concepts, key technologies, developments, and potential trends of bearingless induction motors have been reviewed, with particularly emphasis on the operation principles, motor topologies, mathematical models, and control strategies. Some selected control strategies are also compared. In addition, there are many issues which still need to be investigated, such as the novel motor topologies, advanced control algorithms, and sensor integration and sensorless technologies, as well as reliability technology for specific applications.

Conflict of Interests

The authors declare that there is no conflict of interests regarding the publication of this paper.

Acknowledgment

This work was supported by the National Natural Science Foundation of China under Project nos. 51305170 and 61104016, the National Science Foundation of Jiangsu Province of China under Project no. BK20130515, the China Postdoctoral Science Foundation which funded the project under Project no. 2012M521012, and the Startup Foundation for Advanced Professional Talents of Jiangsu University under Project no. 12JDG057.

References

[1] P. K. Hermann, "A radial active magnetic bearing," London Patent Patent, 1973.

[2] R. Bosch, "Development of a bearingless motor," in *Proceedings of the International Conference of Electric Machines (ICEM '88)*, pp. 373–375, Pisa, Italy, September 1988.

[3] A. Chiba, M. Hanazawa, T. Fukao, and M. Azizur Rahman, "Effects of magnetic saturation on radial force of bearingless synchronous reluctance motors," *IEEE Transactions on Industry Applications*, vol. 32, no. 2, pp. 354–362, 1996.

[4] W. Bu, S. Huang, S. Wan, and W. Liu, "General analytical models of inductance matrices of four-pole bearingless motors with two-pole controlling windings," *IEEE Transactions on Magnetics*, vol. 45, no. 9, pp. 3316–3321, 2009.

[5] L. Chen and W. Hofmann, "Speed regulation technique of one bearingless 8/6 switched reluctance motor with simpler single winding structure," *IEEE Transactions on Industrial Electronics*, vol. 59, no. 6, pp. 2592–2600, 2012.

[6] H. Wang, Y. Wang, X. Liu, and J.-W. Ahn, "Design of novel bearingless switched reluctance motor," *IET Electric Power Applications*, vol. 6, no. 2, pp. 73–81, 2012.

[7] M. Henzel, K. Falkowski, and M. Zokowski, "The analysis of the control system for the bearingless induction electric motor," *Journal of Vibroengineering*, vol. 14, no. 1, pp. 16–21, 2012.

[8] A. Chiba and J. A. Santisteban, "A PWM harmonics elimination method in simultaneous estimation of magnetic field and displacements in bearingless induction motors," *IEEE Transactions on Industry Applications*, vol. 48, no. 1, pp. 124–131, 2012.

[9] X.-D. Sun, H.-Q. Zhu, and W. Pan, "Decoupling control of bearingless permanent magnet-type synchronous motor using artificial neural networks-based inverse system method," *International Journal of Modelling, Identification and Control*, vol. 8, no. 2, pp. 114–121, 2009.

[10] M. Ooshima, A. Chiba, T. Fukao, and M. Azizur Rahman, "Design and analysis of permanent magnet-type bearingless motors," *IEEE Transactions on Industrial Electronics*, vol. 43, no. 2, pp. 292–299, 1996.

[11] K. Inagaki, A. Chiba, M. A. Rahman, and T. Fukao, "Performance characteristics of inset-type permanent magnet bearingless motor drives," in *Proceedings of the IEEE Power Engineering Society Winter Meeting*, pp. 202–207, Singapore, January 2000.

[12] Y. Okada, S. Miyamoto, and T. Ohishi, "Levitation and torque control of internal permanent magnet type bearingless motor," *IEEE Transactions on Control Systems Technology*, vol. 4, no. 5, pp. 565–571, 1996.

[13] Z. Ren, L. S. Stephens, and A. V. Radun, "Improvements on winding flux models for a slotless self-bearing motor," *IEEE Transactions on Magnetics*, vol. 42, no. 7, pp. 1838–1848, 2006.

[14] Z. Ren and L. S. Stephens, "Force characteristics and gain determination for a slotless self-bearing motor," *IEEE Transactions on Magnetics*, vol. 42, no. 7, pp. 1849–1860, 2006.

[15] J. Asama, R. Kawata, T. Tamura, T. Oiwa, and A. Chiba, "Reduction of force interference and performance improvement of a consequent-pole bearingless motor," *Precision Engineering*, vol. 36, no. 1, pp. 10–18, 2012.

[16] J. Asama, M. Amada, N. Tanabe et al., "Evaluation of a bearingless PM motor with wide magnetic gaps," *IEEE Transactions on Energy Conversion*, vol. 25, no. 4, pp. 957–964, 2010.

[17] M. Ooshima and C. Takeuchi, "Magnetic suspension performance of a bearingless brushless DC motor for small liquid pumps," *IEEE Transactions on Industry Applications*, vol. 47, no. 1, pp. 72–78, 2011.

[18] H. Grabner, W. Amrhein, S. Silber, and W. Gruber, "Nonlinear feedback control of a bearingless brushless DC motor," *IEEE/ASME Transactions on Mechatronics*, vol. 15, no. 1, pp. 40–47, 2010.

[19] A. Chiba and T. Fukao, "Optimal design of rotor circuits in induction type bearingless motors," *IEEE Transactions on Magnetics*, vol. 34, no. 4, pp. 2108–2110, 1998.

[20] R. L. A. Ribeiro, F. E. F. Castro, A. O. Salazar, and A. L. Maitelli, "A suitable current control strategy for split-phase bearingless three-phase induction machine," in *Proceedings of the 36th IEEE Power Electronics Specialists Conference*, pp. 701–706, Recife, Brazil, June 2005.

[21] J. Huang, M. Kang, and J.-Q. Yang, "Analysis of a new 5-phase bearingless induction motor," *Journal of Zhejiang University A*, vol. 8, no. 8, pp. 1311–1319, 2007.

[22] A. Chiba, D. Akamatsu, T. Fukao, and M. A. Rahman, "An improved rotor resistance identification method for magnetic field regulation in bearingless induction motor drives," *IEEE Transactions on Industrial Electronics*, vol. 55, no. 2, pp. 852–860, 2008.

[23] J. Santisteban, O. Salazar, R. Stephan, and W. Dunford, "A bearingless machine—an alternative approach," in *Proceedings of the 5th International Symposium on Magnetic Bearings (ISMB '96)*, pp. 345–349, Kanazawa, Japan, August 1996.

[24] X. Sun and H. Zhu, "Artificial neural networks inverse control of 5 degrees of freedom bearingless induction motor," *International Journal of Modelling, Identification and Control*, vol. 15, no. 3, pp. 156–163, 2012.

[25] Z.-Q. Deng, X.-L. Wang, B. Li, L.-G. He, and Y.-G. Yan, "Study on independent control of the levitation subsystem of bearingless induction motors," *Proceedings of the Chinese Society of Electrical Engineering*, vol. 23, no. 9, pp. 107–111, 2003.

[26] Z. Yang, X. Sun, M. Wang, and H. Zhu, "Decoupling control of bearingless induction motors based on least squares support vector machine inverse," *Journal of Computational and Theoretical Nanoscience*, vol. 11, no. 5, pp. 1403–1409, 2014.

[27] U. A. U. Amirulddin, G. M. Asher, P. Sewell, and K. J. Bradley, "Dynamic field modelling of torque and radial forces in vector-controlled induction machines with bearing relief," *IEE Proceedings Electric Power Applications*, vol. 152, pp. 894–904, 2005.

[28] U. A. U. Amirulddin, G. M. Asher, P. Sewell, and K. J. Bradley, "Dynamic field modelling of torque and radial forces in vector-controlled induction machines with bearing relief," *IEE Proceedings-Electric Power Applications*, vol. 152, pp. 894–904, 2005.

[29] A. Laiho, A. Sinervo, J. Orivuori, K. Tammi, A. Arkkio, and K. Zenger, "Attenuation of harmonic rotor vibration in a cage rotor induction machine by a self-bearing force actuator," *IEEE Transactions on Magnetics*, vol. 45, no. 12, pp. 5388–5398, 2009.

[30] Y. He and H. Nian, "Analytical model and feedback control of the levitation force for an induction-type bearingless motor," in *Proceedings of the the 5th International Conference on Power Electronics and Drive Systems*, pp. 242–246, 2003.

[31] Y. Wang, Z.-Q. Deng, and X.-L. Wang, "Direct torque control of bearingless induction motor," *Proceedings of the Chinese Society of Electrical Engineering*, vol. 28, no. 21, pp. 80–84, 2008.

[32] H.-Q. Zhu, Y. Zhou, T.-B. Li, and X.-X. Liu, "Decoupling control of 5 degrees of freedom bearingless induction motors using α-th order inverse system method," *Acta Automatica Sinica*, vol. 33, no. 3, pp. 273–278, 2007.

[33] T. Tera, Y. Yamauchi, A. Chiba, T. Fukao, and M. A. Rahman, "Performances of bearingless and sensorless induction motor drive based on mutual inductances and rotor displacements estimation," *IEEE Transactions on Industrial Electronics*, vol. 53, no. 1, pp. 187–194, 2006.